THE UNIVERSITY OF ALABAMA® | University Libraries

Classifying X-Ray Sources in External Galaxies from X-Ray Colors

J. A. Irwin – University of Michigan
et al.

Deposited 09/14/2018

Citation of published version:

Prestwich, A., et al. (2003): Classifying X-Ray Sources in External Galaxies from X-Ray Colors. *The Astrophysical Journal*, 595(2). DOI: 10.1086/377366/meta

© 2003. The American Astronomical Society. All rights reserved. Printed in U.S.A.

The Astrophysical Journal, 595:719–726, 2003 October 1
© 2003. The American Astronomical Society. All rights reserved. Printed in U.S.A.

CLASSIFYING X-RAY SOURCES IN EXTERNAL GALAXIES FROM X-RAY COLORS

A. H. Prestwich
Harvard-Smithsonian Center for Astrophysics, Cambridge, MA 02138

J. A. Irwin
University of Michigan, 909 Dennison Building, Ann Arbor, MI 48109

R. E. Kilgard, M. I. Krauss, A. Zezas, F. Primini, and P. Kaaret
Harvard-Smithsonian Center for Astrophysics, Cambridge, MA 02138

and

B. Boroson
Center for Space Research, Massachusetts Institute of Technology, Cambridge, MA 02138
Received 2002 June 8; accepted 2003 June 3

ABSTRACT

The X-ray populations of Local Group galaxies have been classified in detail by *Einstein*, *ROSAT*, and *ASCA*, revealing a mix of binaries, supernova remnants (SNRs), and H II regions. However, these observatories were unable to resolve X-ray sources in galaxies beyond the Local Group. With *Chandra*'s exquisite spatial resolution, we are able to resolve sources in a sample of nearby galaxies. We show that there are highly significant differences in the X-ray colors of sources in bulge and disk systems. In particular, we find that there is a population of X-ray–soft, faint sources in disk galaxies not seen in bulges and a smaller population of hard sources also seen preferentially in disk systems. These differences can be used as a basis to classify sources as low- and high-mass X-ray binaries, SNRs, and supersoft sources. We suggest that the soft sources seen preferentially in disks are probably dominated by SNRs, although we cannot rule out the possibility that they are a new population of absorbed, faint, supersoft accretion sources associated with the young stellar population. The hard sources seen in disks but not bulges we identify as high-mass X-ray binaries. While it is impossible to classify any individual source on the basis of X-ray color alone, the observations presented here suggest that it is possible to separate sources into groups dominated by one or two source types. This classification scheme is likely to be very useful in population studies, where it is crucial to distinguish between different classes of objects.

Subject headings: galaxies: spiral — galaxies: starburst — surveys — X-rays: galaxies — X-rays: general

1. INTRODUCTION

Our galaxy and other nearby galaxies contain a multitude of X-ray sources (Fabbiano 1989). Observations of sources in the Milky Way and Local Group galaxies show that many of the brightest X-ray sources are high- and low-mass X-ray binaries (HMXBs, LMXBs), but there are also sources associated with supernova remnants (SNRs) and H II regions. For example, the *ROSAT* survey of M31 (Supper et al. 2001) revealed a total of 560 X-ray sources, 16 of which have been optically identified with SNRs and 33 with globular clusters. Most of the bulge sources in M31 have been identified on the basis of their X-ray spectra as low-mass X-ray binaries (Trinchieri et al. 1999; Primini, Forman, & Jones 1993). Studies of X-ray populations in a wide range of galaxies is potentially very valuable. For example, since X-ray binaries are products of the endpoint of stellar evolution, the X-ray binary population should be related to the history of star formation in each galaxy (Wu 2001; Kilgard et al. 2003). However, the resolution of *Einstein*, *ROSAT*, and *ASCA* was not sufficient to allow identification of sources in galaxies beyond the Local Group. *Chandra* has the angular resolution necessary to study the X-ray source population in more distant galaxies for the first time (Blanton, Sarazin, & Irwin 2001; Tennant et al. 2001; Irwin, Sarazin, & Bregman 2002; Fabbiano, Zezas, & Murray 2001; Soria & Wu 2002).

In this paper, we compare X-ray populations of a sample of disk and bulge galaxies. We show that there is a highly significant difference in the X-ray colors of sources in bulge and disk systems. Disk galaxies have a population of soft sources and a population of hard sources not seen in bulges. X-ray colors are known to be a sensitive discriminator of source type (White & Marshall 1984; Haberl et al. 2000; Yokogawa et al. 2000; Sasaki, Haberl, & Pietsch 2000), and we interpret these differences as differences in the source population. Furthermore, we suggest that X-ray colors derived from *Chandra* observations can be used to identify different classes of X-ray sources in nearby galaxies. In § 2, we describe our data analysis. In § 3, we show the difference in the distribution of X-ray colors in bulge and disk systems, and in § 4, we suggest a classification scheme based on colors. In § 5, we discuss the effects of absorption on source classification, and in § 6, we discuss the spatial distribution, luminosities, and variability characteristics of the different classes of sources. Finally, in § 7, we summarize our results and give suggestions for further work.

2. DATA ANALYSIS

Our sample for this study consists of two late-type face-on spiral galaxies (M101 and M83) and three elliptical/bulge systems (NGC 4697, the inner bulge of M31, and the bulge of NGC 1291). Observations of all galaxies were

TABLE 1
PROPERTIES OF OBSERVATIONS AND GALAXIES

Galaxy	Hubble Type	Observation Identification	Date	Exposure (s)	n_H (10^{20} cm^{-2})	Distance (Mpc)	L_{min}	N(background)	N(source)
NGC 1291.....	S0/a	2059	2000 Nov 7	22906	2.24	8.6	4.4E37	3	44
M83	Sc	793	2000 Apr 29	48562	3.70	4.7	7.1E36	6	122
M83	Sc	2064	2001 Sep 4	7207	3.70	4.7	4.8E37	1	38
M31	SA	309	2000 Jun 1	4942	6.68	0.7	1.7E36	1	...
NGC 4697.....	E6	784	2000 Jan 15	39013	2.14	23.3	2.0E38	5	66
M101	SAB	934	2000 Mar 26	97602	1.15	5.4	3.7E36	10	113
M101	SAB	2065	2000 Oct 29	9583	1.15	5.4	3.8E37	1	10

performed on the back-illuminated ACIS-S3 CCD. All analysis was performed using the *Chandra* Interactive Analysis of Observations software package (CIAO) v2.2.1 and the *Chandra* Calibration Database v2.10. Data were screened for times of high background, as many of the observations occurred near periods of solar activity. Exposure times of the screened observations are in Table 1. Source lists were constructed using *wavdetect* (Freeman et al. 2002), the Mexican-hat wavelet source detection routine that is part of CIAO. We ran *wavdetect* on 0.3–6.5 keV band images using wavelet scales of 2, 4, 8, and 16 pixels. This combination of energy band and wavelet scales yielded the fewest spurious detections and found all visually obvious point sources. The default value of the parameter sigthresh (1×10^{-6}) was used to identify source pixels. The output source regions were visually inspected to identify multiple detections and single sources detected twice. Nuclear sources were removed from the source lists. Sources outside of the ACIS-S3 chip were excluded from further analysis. Sources outside the optical boundaries of the galaxy, defined as the observed diameter at 25 mag arcsec^{-2} in the blue band, D_{25}, were also excluded, since these have a high probability of being background objects. Values for D_{25} were taken from Tully (1988). Table 1 gives the total number of sources detected in each galaxy with a minimum of 20 net counts and significance greater than 4 σ (see § 3) and the expected number of background sources (same significance) from the log N–log S curves of Giacconi et al. (2001). Variations in the number of background sources with position on the sky (Cowie et al. 2002) will change the number of expected background sources by, at most, a factor of 3.

The total number of counts for each detected source were calculated in three bands: the soft band (0.3–1 keV), medium band (1–2 keV), and hard band (2–8 keV). Counts were extracted from source regions determined by 4 σ source ellipses from *wavdetect*. This overestimates the source size, but the contribution from background is negligible. The background region for each source was taken to be an ellipse with major and minor axes equal to 4 times the source axes and excluding the source region and any other overlapping source regions. Background ellipse radii were not allowed to exceed 50 pixels (about 25″) to avoid contamination from variations in the diffuse emission. Source count rates were corrected using monochromatic exposure maps created for each band using a monochromatic response at the mean photon energy in each band: 0.65 keV (soft band), 1.5 keV (medium band), and 5 keV (hard band). These maps take into account vignetting and spatial variation of the CCD QE. X-ray colors were then calculated for each source as H1 = $(M - S)/T$ (soft) and H2 = $(H - M)/T$ (hard), where S, M, and H are the counts in the soft, medium, and hard bands, respectively, and T is the total counts in all three bands combined.

We estimated fluxes from each source assuming a 5 keV thermal bremsstrahlung model with photoelectric absorption. The n_H was fixed at the Galactic value. No correction for absorption in the host galaxy was applied. Luminosities were derived in the 0.3–8 keV band using distances from the Nearby Galaxies Catalog (Tully 1988), which assumes $H_0 = 75$ km s^{-1} Mpc^{-1} coupled with a Virgo infall model. A more detailed description of the data analysis, discussing the relevant biases and presenting source lists with spectral and timing results, will be presented in R. E. Kilgard et al. (2003, in preparation).

3. COLOR DIFFERENCES BETWEEN BULGE AND DISK SOURCES

Figure 1 shows the X-ray color-color diagram for sources in the inner bulge of M31 and the disk of M101. Only sources with a minimum of 20 net counts and significance

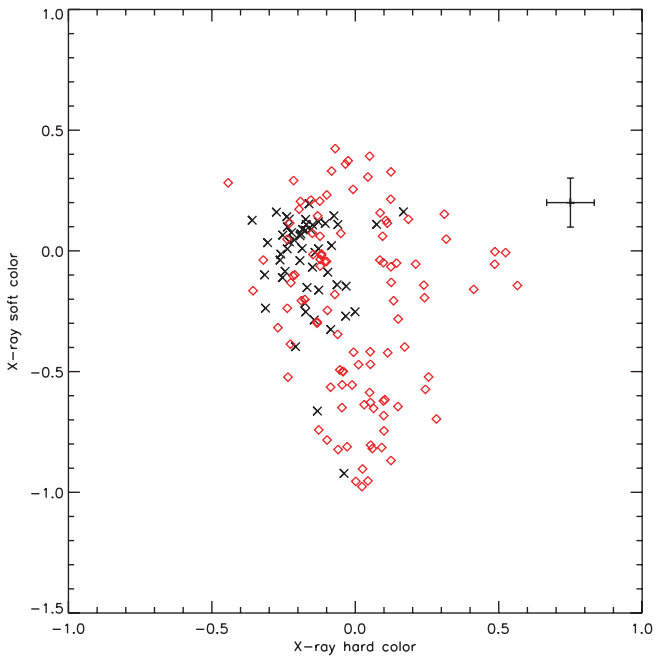

FIG. 1.—X-ray hard color (x-axis) plotted against X-ray soft color for the inner bulge of M31 (*crosses*) and the disk of M101 (*diamonds*). X-ray hard color is defined as H2 = $(H - M)/T$, X-ray soft color as H1 = $(M - S)/T$.

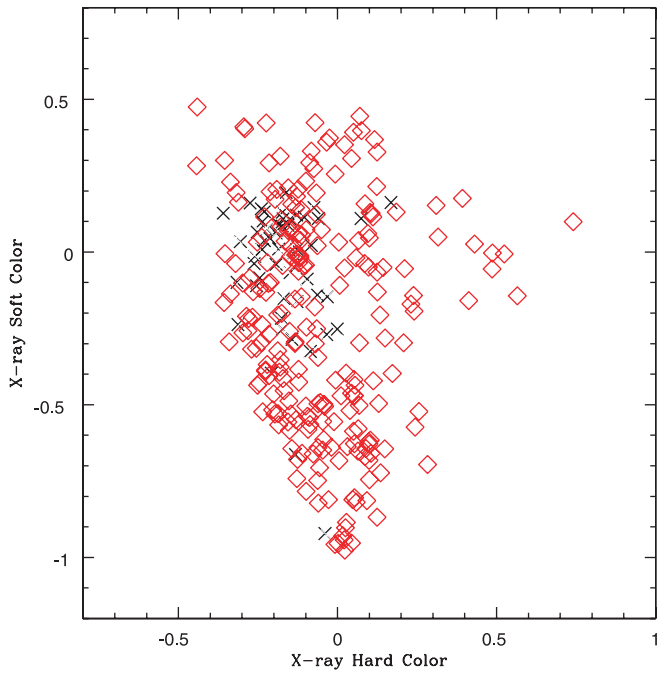

FIG. 2.—X-ray hard color (x-axis) plotted against X-ray soft color for a selection of bulge and disk systems. *Red diamonds*: Sources from the disk galaxies M101 and M83. *Black crosses*: Sources from bulge systems (inner bulge of M31, bulge of NGC 191, and the elliptical NGC 4697). X-ray hard color is defined as $H2 = (H - M)/T$, X-ray soft color as $H1 = (M - S)/T$.

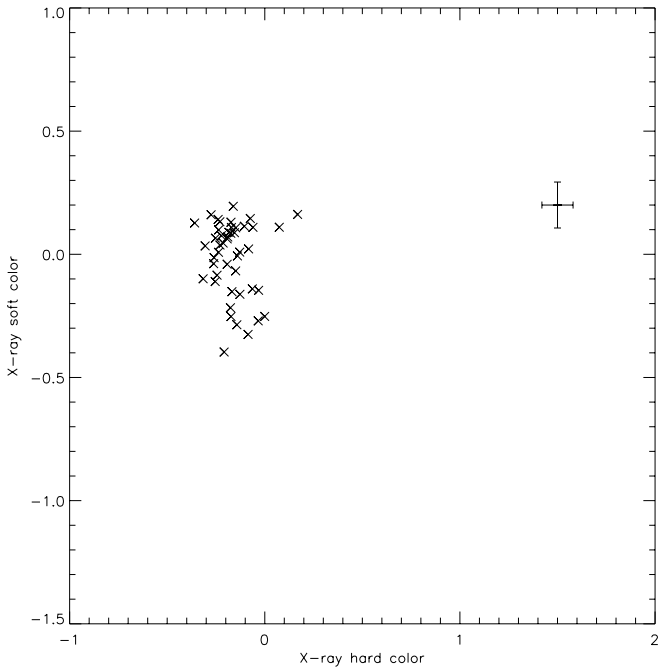

FIG. 3.—X-ray color-color diagram for LMXBs in M31. X-ray hard color is defined as $H2 = (H - M)/T$, X-ray soft color as $H1 = (M - S)/T$.

greater than 4 σ are plotted and used in subsequent analysis. There is a clear difference in the colors of sources in M31 and M101. The bulge sources in M31 are clustered in a relatively narrow color range, with both H1 and H2 having values between -0.4 and 0.4. The M101 disk sources, on the other hand, have a tail of soft sources extending to $H1 = -1$. M101 also has a population of sources with $H1 > 0.1$ not seen in M31. It is important to note that the M31 exposure is deeper than the M101 observation (see Table 1). The approximate luminosity limit for sources with $\geq$20 counts in M31 is nearly a factor of 2 lower than for sources in M101. Hence, if the extra soft and hard sources existed in M31, they should have been detected.

Figure 2 shows the X-ray color-color diagram for sources drawn from a larger sample of galaxies (the bulges of M31 and NGC 1291, the elliptical galaxy NGC 4697, and the disk galaxies M83 and M101). The sources were selected according to the criteria described in the previous paragraph. The color differences between disk and bulge sources in this larger sample are very clear and highly significant. A Kolmogorov-Smirnov (K-S) test gives the probability that the two data sets arise from the same distribution as 2.5×10^{-7} (soft color) and 9.5×10^{-5} (hard color).

4. CLASSIFICATION OF SOURCES

The differences in the colors between bulge and disk sources indicates a difference in the source population and can be used classify the sources in different systems. While it is impossible to classify any individual source with confidence on the basis of X-ray colors alone, it is valuable to be able to separate sources in a statistical sense for population studies.

As mentioned in § 1, the bulge of our Galaxy and M31 as well as sources in elliptical galaxies are dominated by low-mass X-ray binaries (Fabbiano 1989; Grimm, Gilfanov, & Sunyaev 2001). We therefore suggest that the region of the X-ray color-color diagram populated by bulge sources contains many LMXBs. The bulge sources are in a region of the diagram characterized by a simple power-law slope (photon index 1–2.5) with some intrinsic (to the source) absorption. This is typical of LMXBs (White, Nagase, & Parmar 1995). The LMXB region is best defined in Figure 3. By cross-correlating our M31 inner bulge source list with the list given by Kong et al. (2002), we have rejected known foreground and background sources, supersoft sources, and sources for which there may be a contribution from hot gas (e.g., those associated with planetary nebula). The resulting plot is illustrative of the intrinsic dispersion in the color-color diagram of LMXBs. Very few of the soft or hard sources described in § 3 and associated with disk regions are likely to be LMXBs. The LMXB area is shown in Figure 4. Figure 4 also shows the predicted colors of power-law spectra with increasing photon index (blue arc). The effect of adding absorption to a simple power law is illustrated with the vertically rising blue lines.

The soft sources (H1 between -0.4 and -0.9) that appear almost exclusively in disks may be identified as thermal SNRs. SNRs are found in regions of ongoing star formation, and hence, very few are found in elliptical galaxies. Thermal SNRs also have soft spectra (Long et al. 1996), consistent with the colors seen here. This is demonstrated in Figure 4. The purple boxes show the colors of several known thermal SNRs in the Small Magellanic Cloud with spectra measured by *ASCA* (Yokogawa et al. 2000). Most of these sources lie below the LMXB region, in the part of the diagram populated by soft sources. One absorbed SNR has $H1 = -0.3$. Additional evidence that these sources are

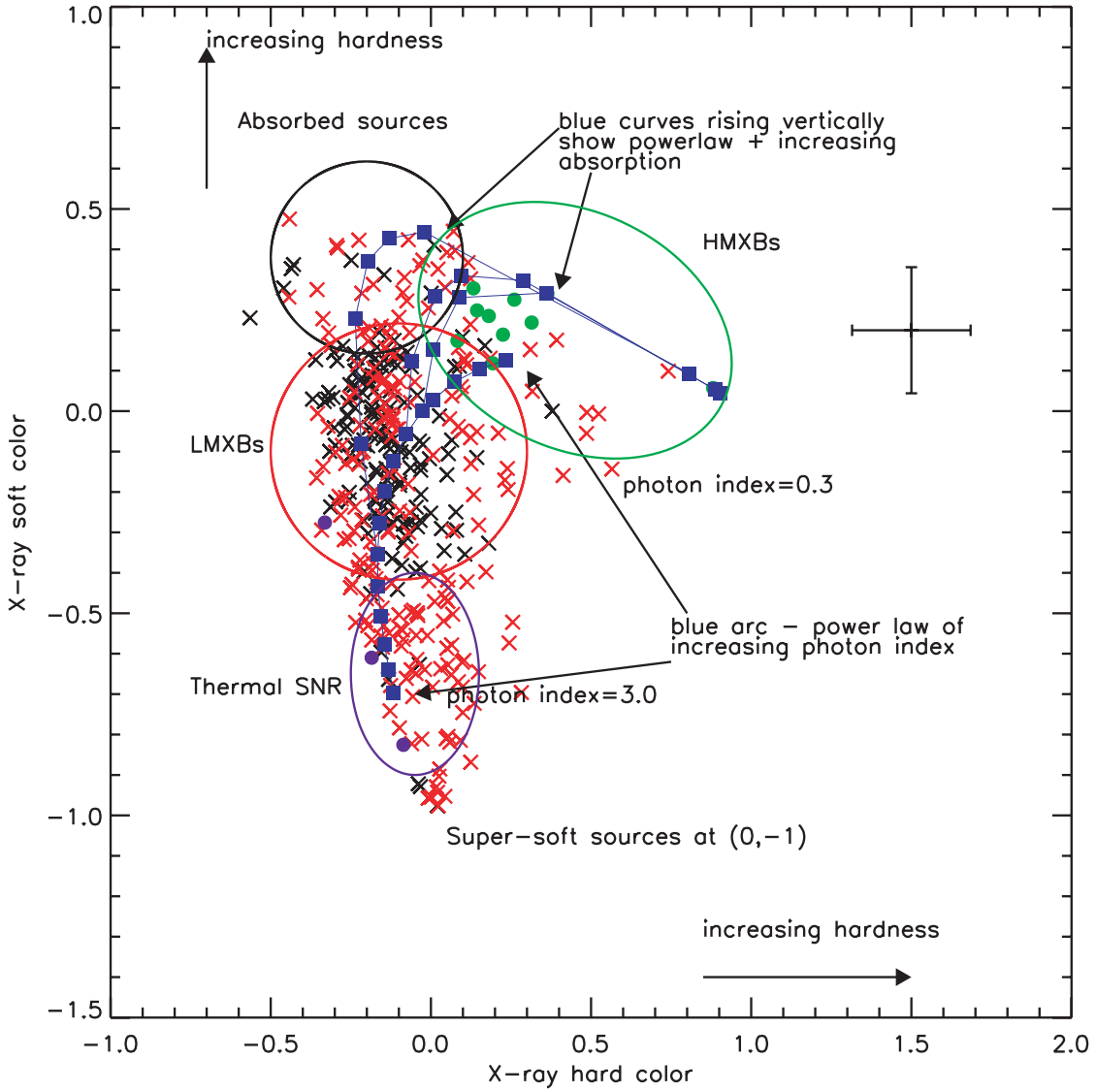

FIG. 4.—Proposed classification scheme. *Red circle*: Area of the color-color diagram that is probably dominated by LMXBs. *Blue ellipse*: Region occupied by thermal SNR. *Green ellipse*: Region occupied by HMXBs. *Black circle*: Most absorbed sources, probably a mixture of types. *Blue arc of points stretching from* (0.3, 0.15) *to* (−0.1, −0.7): Colors of a simple power-law spectral model with photon index increasing from 0.7 to 3.0. *Blue curves rising vertically*: Effect of adding absorption to power-law slopes of photon index 1.0, 1.2, and 2.0.

indeed thermal SNR comes from a detailed study of the discrete source population in M83 by Soria & Wu (2003). They find that two of the brightest soft sources have X-ray spectra dominated by emission lines, typical of SNR. However, it is important to stress that some of these soft-disk sources may be absorbed supersoft sources (see discussion below). SNRs dominated by nonthermal emission (Crab-like objects) may also contribute to the source population. These will have spectra somewhat harder than thermal SNRs and will probably be located in the LMXB or absorbed sources part of the diagram.

There are a handful of sources with H2 > 0 that appear in the disks but not in the bulges. The most natural interpretation of these sources is that they are high-mass X-ray binaries. High-mass X-ray binaries have high-mass (hence, short-lived) secondaries and are typically found in regions of active star formation. They are known to have hard spectra in the 1–10 keV region, with a power-law photon index of 1–2 and often high variable intrinsic absorption (White, Nagase, & Parmar 1995). The green circles in Figure 4 show the colors of known binary pulsars observed by *ASCA* (Yokogawa et al. 2000). As noted above, most known HMXBs are associated with pulsars in binary systems. Therefore, the HMXBs shown in Figure 4 represent only pulsed (neutron star) binaries and not black hole binaries with early-type companions. These sources have spectra similar to black hole LMXB companions (van Paradijs 1999) and probably are not well separated from black hole LMXB sources in the color-color diagram.

There are a small number of sources with H2 $= 0$ and H1 $= -1$. These sources essentially have no counts above 1 keV, and some are undoubtedly classical supersoft sources (Greiner, Hasinger, & Kahabka 1991). These supersoft sources seem to occur in both bulge and disk systems. They are frequently brighter than the sources identified as SNRs, and most are variable (see § 6). Pence et al. (2001) have

identified 10 sources in M101 as supersoft. We do not include six of these fainter sources because they have less than 20 counts. We detect the remaining four sources, three of which have H1 ≤ -0.9 and one of which has H1 $= -0.81$. It is also possible that some (or even all) of the soft sources identified as thermal SNRs are absorbed supersoft sources. Absorption will decrease the flux in the lowest energy *Chandra* band, shifting the soft color vertically upward on the color-color plot (see § 5). If this is the case, we have identified a new population of faint, absorbed, accretion-powered soft sources in disk galaxies, probably associated with the young stellar population. We favor the hypothesis that the soft source population is dominated by SNRs, but a new population of accretion-powered soft sources cannot be ruled out. An in-depth study of the variability and spectral characteristics of the soft sources (see § 6) is required to distinguish between these two models.

5. ABSORPTION AND OVERLAP IN SOURCE TYPE

There will undoubtedly be some overlap in source type in the color-color diagram, because both different sources have intrinsically similar spectra (e.g., black hole binaries with high- and low-mass companions) and because of absorption.

Photons in the lowest energy *Chandra* band will be preferentially removed in an absorbed source, making H1 harder. This will move the source vertically up the color-color diagram, as illustrated in Figure 4. When the absorption becomes very severe ($n_{\rm H} \sim 10^{22}$), photons in the medium *Chandra* band will also be removed, causing H2 to become harder. The source will then curve to the right in Figure 4, as shown by the tracks of increasing absorption. Absorption will cause supersoft sources to be confused with SNRs, move SNRs into the LMXB region of the diagram, and blur the distinction between LMXBs and HMXBs. Color information in the *Chandra* bands will be very limited for highly inclined galaxies, where essentially all low-energy photons are lost. In this case, sources distinguished primarily on the basis of their soft color will be confused (SNRs, supersoft sources, LMXBs), and only a very rough separation on the basis of hard color will be possible.

6. LUMINOSITIES, VARIABILITY, AND SPATIAL DISTRIBUTION

The soft sources identified in § 4 as SNRs have considerably less scatter in their luminosities than do sources with H1 > -0.6, i.e., a higher fraction of the sources in the LMXB part of the diagram have luminosities greater than 10^{37} ergs s^{-1}. This is demonstrated in Figure 5. The left panel shows the soft X-ray color plotted as a function of luminosity for M101 and M83. This difference in the distribution of luminosities in LMXB and soft sources is significant: a K-S test gives the probability that they are drawn from the same distribution as 6×10^{-4}. The larger scatter in the luminosities of sources with H1 > -0.5 is naturally explained if many of these objects are accreting binaries. Binaries can reach much higher luminosities (especially in a flare state) than is typically observed in evolved SNRs (10^{36}–10^{37} ergs s^{-1}). The X-ray luminosities of the soft sources are typical of brighter SNRs: there are certainly other soft sources below our detection threshold. Several of the brightest soft sources have very extreme colors (H1 $= -1$) and have colors and luminosities characteristic of supersoft sources (Kahabka, Pietsch, & Hasinger 1994). These are probably accretion-powered.

The right panel of Figure 5 shows the luminosity plot for X-ray hard color. This plot suggests that sources with the hardest colors (H2 ≥ 0.2, HMXB candidates) have smaller scatter than less extreme sources. A K-S test shows that the luminosity distributions of the hardest sources is significantly different from those in the LMXB part of the diagram. The probability that they are drawn from the same

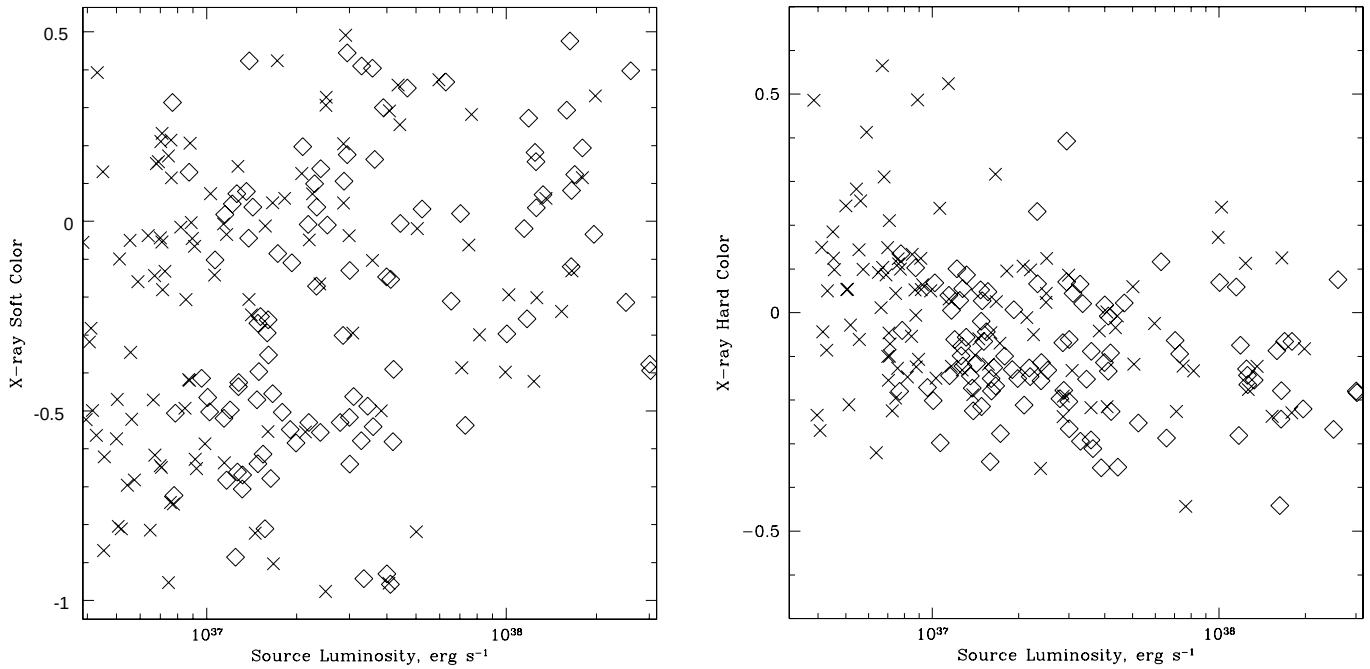

FIG. 5.—Source luminosity plotted against X-ray soft color (*left*) and X-ray hard color (*right*) for M101 (*crosses*) and M83 (*diamonds*)

distribution is 5×10^{-5}. The luminosity function of LMXB sources in the Milky Way extends to higher luminosities than the HMXB luminosity function (Grimm et al. 2001), consistent with what is observed here. We note, however, that extremely luminous sources tentatively associated with HMXBs are seen in starburst galaxies (Zezas & Fabbiano 2003; Fabbiano et al. 2001; Prestwich 2001).

If the soft sources discussed in § 4 are SNRs, they should show little or no evidence for variability. When SNRs are young ($\leq$1000 yr), several emission mechanisms might contribute to the X-ray emission, and the flux may be variable (Schlegel 1995). However, once the remnant enters the adiabatic phase, the luminosity should decline gradually (Jones, Smith, & Straka 1981; Hamilton, Chevalier, & Sarazin 1983). In contrast, accretion-powered supersoft sources are known to be variable (Kahabka, Pietsch, & Hasinger 1994; Kong et al. 2002), and detection of variability in a large fraction of the soft sources would support the hypothesis that they are accretion-powered. Both M101 and M83 have one deep exposure in the *Chandra* archive, with a second shorter observation (see Table 1). The second shorter exposure of M83 was taken 16 months after the first, and the second exposure of M101 taken 7 months after the first. In the long (100 ks) pointing of M101, there are 28 soft sources (potential SNRs) detected. Most of these have 20–100 counts and are not detected in the short (10 ks) observation. This does not provide very stringent constraints on the variability of the soft sources, since to be detected in the short observation, they would have to increase in flux by factors of 5–10. There are two soft sources detected in both the long and short observation. One source with $H1 = -0.8$ shows no evidence for variability. Another source is significantly variable and has a $H1 = -0.78$ in the long observation. This source has a luminosity of $\sim 10^{39}$ ergs s^{-1} and is the brightest object in M101 (source 98 from Pence et al. 2001). It is highly variable and is clearly an accretion source. Two hard (possible HMXB) sources are detected in both observations in M101. One has $H2 = 0.31$ in the long observation and shows no evidence for variability. One source has $H2 = 0.48$, and the flux approximately doubles in the second observation.

There are 28 soft (possible SNR) sources detected in M83 in the long (50 ks) observation. A total of seven sources with soft colors that were detected in the long observation were also detected in the short observation. Two of these are clearly variable, while the remaining five have approximately constant flux. Of the 28 soft sources detected in the long observation, five sources should have been detected in the short (10 ks) observation, assuming no variability. Three of these have extremely soft colors, are clearly variable, and are probably supersoft sources. The remaining two sources may have declined in flux between the two observations. Three hard (potentially HMXB) sources were detected in the long observation of M83. One of these sources may be variable. We conclude that we have insufficient data to make definitive statements about the variability properties of the soft sources in either M83 or M101.

The spatial distribution of the soft (*yellow crosses*) and LMXB (*red crosses*) sources is shown in Figure 6 for M83. The *Chandra* X-ray image is shown on the left, and the *U*-band optical image on the right. Both LMXB and soft sources have a tendency to occur in the spiral arms. The main difference between the two distributions, however, is that the nuclear X-ray sources are almost all sources with LMXB colors. In M101, the X-ray sources follow a similar pattern (see also Pence et al. 2001), with both types of sources following the spiral structure. There is only a single diffuse source at the center of M101 (there is essentially no bulge in this system), so segregation of central sources is not seen.

7. SUMMARY AND CONCLUSIONS

In this paper, we show that there is a highly significant difference in the X-ray colors of sources in bulge and disk systems. Disk galaxies have an additional population of soft X-ray sources and a scattering of hard sources not seen in bulge systems. The hard disk sources are probably HMXBs. The soft disk sources are probably dominated by SNRs, but we cannot rule out a contribution from a new population of soft, faint, absorbed accretion sources associated with the young stellar population.

The differences in X-ray colors of sources in nearby disk and bulge galaxies can be used as a starting point for source classification, with the color-color diagram approximately separating SNR, LMXB, and HMXB sources. These conclusions are strengthened by the location of known thermal SNRs and binary pulsars in the X-ray color-color diagram. The luminosities of sources identified as SNRs and HMXBs are consistent with what is observed in the Galaxy (Grimm et al. 2001). The variability characteristics of different classes of sources should provide additional constraints on their nature. Accreting binaries are likely to vary stochastically, while the flux from thermal SNR should remain constant. Unfortunately, although there are two *Chandra* observations for both disk galaxies (M101 and M83), the second observations are not deep enough to effectively constrain the variability of the soft sources identified as SNRs.

It is not possible to identify a source on the basis of X-ray color alone. However, separating sources on the basis of X-ray colors will be very valuable for population studies. Although X-ray colors provide an excellent starting point for the classification of sources in nearby galaxies, there is some overlap in source type in the X-ray color-color diagram. For example, SNRs that are very highly absorbed will move vertically upward into the LMXB part of the color-color diagram. The population of soft sources may contain some supersoft sources or X-ray binaries with soft spectra. Therefore, other information, such as source variability, luminosity, and optical counterparts as well as position within the galaxy must be used to complete the classification process. Deeper *Chandra* images of nearby galaxies are required to investigate the variability and spectral properties of the different source classes outlined here.

Thanks to Harvey Tananbaum for improving the first draft of this paper, Randall Smith for his help with SLANG scripting, and Rosanne Di Stefano and Roberto Soria for stimulating discussions. This work was supported by NASA contract NAS 8-39073 (CXC) and GO1-2029A.

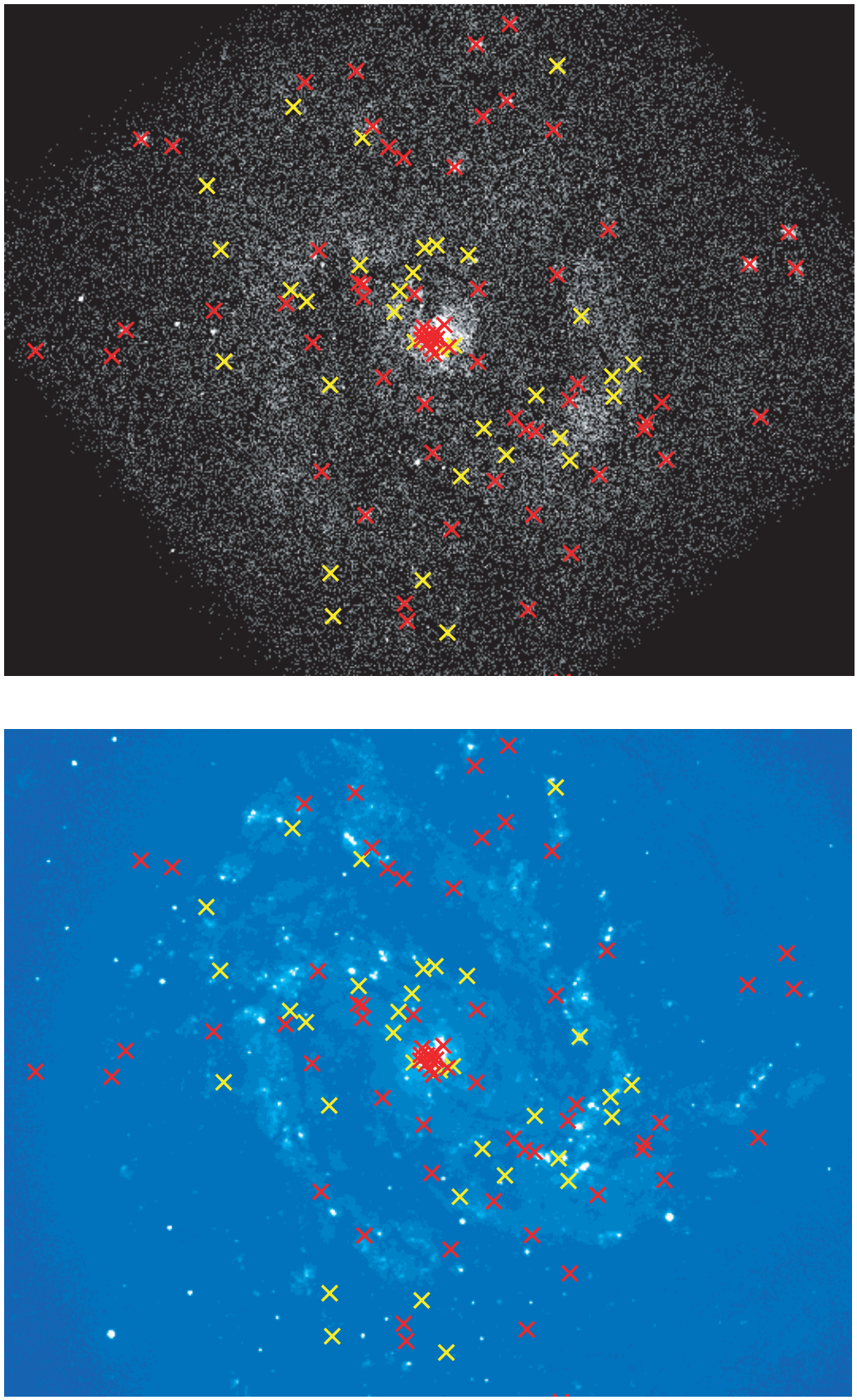

FIG. 6.—M83 X-ray sources plotted on the *Chandra* image (*left*) and *U*-band image (*right*). *Red crosses*: Sources whose colors make them good candidates for LMXBs. *Yellow crosses*: Soft sources (possible SNRs).

REFERENCES

Blanton, E. L., Sarazin, C. L., & Irwin, J. A. 2001, ApJ, 552, 106
Cowie, L. L., Garmire, G. P., Bautz, M. W., Barger, A. J., Brandt, W. N., & Hornschemeier, A. E. 2002, ApJ, 566, L5
Fabbiano, G. 1989, ARA&A, 27, 87
Fabbiano, G., Zezas, A., & Murray, S. S. 2001, ApJ, 554, 1035
Freeman, P. E., Kashyap, V., Rosner, R., & Lamb, D. Q. 2002, ApJS, 138, 185
Giacconi, R., et al. 2001, ApJ, 551, 624
Greiner, J., Hasinger, G., & Kahabka, P. 1991, A&A, 246, L17
Grimm, H.-J., Gilfanov, M., & Sunyaev, R. 2001, A&A, 391, 923
Haberl, F., Filipović, M. D., Pietsch, W., & Kahabka, P. 2000, A&AS, 142, 41
Hamilton, A. J. S., Chevalier, R. A., & Sarazin, C. L. 1983, ApJS, 51, 115
Irwin, J. A., Sarazin, C. L., & Bregman, J. N. 2002, ApJ, 570, 152
Jones, E. M., Smith, B. W., & Straka, W. C. 1981, ApJ, 249, 185
Kahabka, P., Pietsch, W., & Hasinger, G. 1994, A&A, 288, 538
Kilgard, R. E, Kaaret, P., Krauss, M. I., Prestwich, A. H., Raley, M. T., & Zezas, A. 2002, ApJ, 573, 138
Kong, A. K. H., Garcia, M. R., Primini, F. A., Murray, S. S., Di Stefano, R., & McClintock, J. E. 2002, ApJ, 577, 738
Long, K. S., Charles, P. A., Blair, W. P., & Gordon, S. M. 1996, ApJ, 466, 750
Pence, W. D., Snowden, S. L., Mukai, K., & Kuntz, K. D. 2001, ApJ, 561, 189
Prestwich, A. 2001, High-Energy Universe at Sharp Focus: *Chandra* Science, E15
Primini, F. A., Forman, W., & Jones, C. 1993, ApJ, 410, 615
Sasaki, M., Haberl, F., & Pietsch, W. 2000, A&AS, 143, 391
Schlegel, E. M. 1995, Rep. Prog. Phys., 58, 1375
Soria, R. & Wu, K. 2002, A&A, 384, 99
Supper, R., Hasinger, G., Lewin, W. H. G., Magnier, E. A., van Paradijs, J., Pietsch, W., Read, A. M., & Trümper, J. 2001, A&A, 373, 63
Tennant, A. F., Wu, K., Ghosh, K. K., Kolodziejczak, J. J., & Swartz, D. A. 2001, ApJ, 549, L43
Trinchieri, G., Israel, G. L., Chiappetti, L., Belloni, T., Stella, L., Primini, F., Fabbiano, P., & Pietsch, W. 1999, A&A, 348, 43
Tully, R. B. 1988, Nearby Galaxies Catalog for Cambridge and New York (Cambridge: Cambridge Univ. Press)
Van Paradijs, J. 1999, in the Many Faces of Neutron Stars, ed. R. Buccheri, J. van Paradijs, & M. A. Alpar (Dordrecht: Kluwer), 279
White, N. E., & Marshall, F. E. 1984, ApJ, 281, 354
White, N. E., Nagase, F., & Parmar, A. N. 1995, in X-Ray Binaries, ed. W. G. H. Lewin, J. van Paradijs, & E. P. J. van den Heuvel (Cambridge: Cambridge Univ. Press), 1
Wu, K. 2001, Publ. Astron Soc. Australia, 18, 443
Yokogawa, J., Imanishi, K., Tsujimoto, M., Nishiuchi, M., Koyama, K., Nagase, F., & Corbet, R. H. D. 2000, ApJS, 128, 491
Zezas, A., & Fabbinao, G. 2002, ApJ, 577, 726